Synthesis and Structure of Di-μ-oxo Nitridotechnetium(VI) Dimers and a Monomeric Nitridotechnetium(V) Mixed-ligand Complex *

John Baldas, John F. Boas, Silvano F. Colmanet and Geoffrey A. Williams
Australian Radiation Laboratory, Lower Plenty Road, Yallambie, Victoria 3085, Australia

The di-μ-oxo technetium(VI) complexes $[\{TcN(S_2CNEt_2)\}_2(\mu\text{-}O)_2]$ **1**, $[\{TcN(S_2CNC_4H_8)\}_2(\mu\text{-}O)_2]$ **2**, $[AsPh_4]_2[\{TcN(CN)_2\}_2(\mu\text{-}O)_2]$ **4** and $[AsPh_4]_2[\{TcN(edt)\}_2(\mu\text{-}O)_2]$ **5** (H_2edt = ethane-1,2-dithiol) have been prepared either by reaction of $[\{TcN(OH_2)_3\}_2(\mu\text{-}O)_2]^{2+}$ or $Cs_2[TcNCl_5]$ in $Na_4P_2O_7$ solution with the appropriate ligand. The ESR spectra of solutions of **1** and **2** in $SOCl_2$ and of **4** in MeCN with added $AsPh_4Cl$·HCl showed that cleavage of the dimer occurs to give the nitridotechnetium(VI) monomers $[TcNCl_2(S_2CNR_2)]$ (R = Et or $R_2 = C_4H_8$) or $[TcNCl_2(CN)_2]^-$. Reaction of $[Tc^{VI}NCl_2(S_2CNEt_2)]$ with $K_2[SCOCOS]$ gave the mixed-ligand complex $[AsPh_4][Tc^{V}N(S_2CNEt_2)(SCOCOS)]$ **3**. Single-crystal X-ray structures (Cu-Kα radiation) were determined for **1**, **2** and **3**. Complexes **1** and **2** are dimeric and are best described as two edge-sharing square pyramids, with Tc≡N and Tc–Tc distances of 1.623(4), 1.624(4), 2.543(1), and 1.65(2), 1.59(2) and, 2.542(2) Å for **1** and **2** respectively. Complex **3** is monomeric with the technetium atom having a square pyramidal geometry, and a Tc≡N distance of 1.54(2) Å.

Mono- and di-meric oxo complexes are a characteristic feature of the chemistry of molybdenum(V). Numerous complexes containing the MoO^{3+}, $[OMo\text{–}O\text{–}MoO]^{4+}$ and $[OMo(\mu\text{-}O)_2\text{-}MoO]^{2+}$ cores have been prepared and structurally characterised.[1-3] We have recently reported that the chemistry of $Tc^{VI}N$ closely parallels that of the isoelectronic $Mo^{V}O$.[4] This is exemplified by the identification of the aquanitrido cation $[(H_2O)_3NTc^{VI}(\mu\text{-}O)_2Tc^{VI}N(OH_2)_3]^{2+}$, which is the analogue of the well established $[Mo_2O_4(OH_2)_6]^{2+}$ cation.[5] The $[NTc^{VI}\text{–}O\text{–}Tc^{VI}N]^{4+}$ core has been established in the cyclic tetramer $[AsPh_4]_4[Tc_4N_4O_2(ox)_6]$ [ox = oxalate(2−)][6] and a preliminary account of the crystal structure of $[\{TcN(S_2CNEt_2)\}_2(\mu\text{-}O)_2]$ **1** has been reported.[5] Comparable oxygen-bridged nitrido complexes have not been reported for any other transition metal. In view of the novelty of these $Tc^{VI}N$ dimeric cores, we now report full structural details for **1** and for the pyrrolidinyl analogue $[\{TcN(S_2CNC_4H_8)\}_2(\mu\text{-}O)_2]$ **2** (NC_4H_8 = pyrrolidinyl). Also reported are chemical and ESR studies of the cleavage of the $NTc(\mu\text{-}O)_2TcN$ system and the preparation and structure of the mixed-ligand complex $[AsPh_4][Tc^{V}N(S_2CNEt_2)(SCOCOS)]$ **3**.

Experimental

Ammonium [^{99}Tc]pertechnetate was supplied by Amersham International plc. Fourier-transform infrared (FTIR) spectra (4000–250 cm^{-1}) were recorded for KBr discs on a Digilab FTS7 spectrophotometer and UV/VIS spectra in MeCN solution. Technetium analyses were performed by liquid scintillation counting after decolorisation of the solution by the addition of H_2O_2. Other analyses were performed by Chemical and Microanalytical Services, Melbourne. Compounds $Cs_2[TcNCl_5]$[7] and $[AsPh_4]_4[Tc_4N_4O_2(ox)_6]$[6] were prepared as previously described.

Preparations.—$[\{TcN(S_2CNEt_2)\}_2(\mu\text{-}O)_2]$ **1**. The brown precipitate of $[Tc_2N_2O_2(OH)_2(OH_2)_2]$ obtained from the hydrolysis of $Cs_2[TcNCl_5]$[4] (70 mg, 0.126 mmol) was collected by centrifugation, washed with water and dissolved in 1 mol dm^{-3} aqueous toluene-*p*-sulfonic acid (3 cm^3) to give an orange-yellow solution, to which was added $Na[S_2CNEt_2]\cdot 3H_2O$ (42 mg, 0.186 mmol), in one lot, dissolved in 1 mol dm^{-3} K_2HPO_4 (4 cm^3). Extraction of the mixture with CH_2Cl_2 and silica gel chromatography with CH_2Cl_2 as eluent gave $[Tc^{V}N(S_2CNEt_2)_2]$ (7.6 mg, 15% yield) and complex **1** (12.9 mg, 37% yield). Recrystallisation of **1** from MeCN gave bright yellow crystals, m.p. 231 °C (decomp.) (Found: C, 21.70; H, 3.55; N, 9.95; O, 5.50; S, 23.05; Tc, 35.40. $C_{10}H_{20}N_4O_2S_4Tc_2$ requires C, 21.65; H, 3.65; N, 10.10; O, 5.75; S, 23.15; Tc, 35.70%). IR: 2981m, 1532vs, 1455s, 1439s, 1355s, 1280s, 1202s, 1152s, 1079m, 1061vs (Tc=N), 1054s (Tc≡N), 996m, 913m, 845m, 779m, 704s, 456m and 384s cm^{-1}. UV/VIS: λ_{max}/nm *ca.* 316(sh).

$[\{TcN(S_2CNC_4H_8)\}_2(\mu\text{-}O)_2]$ **2**. To a saturated aqueous solution of $Na_4P_2O_7\cdot 10H_2O$ (3 cm^3) was added $Cs_2[TcNCl_5]$ (70 mg, 0.126 mmol) and the mixture shaken and warmed until the solid completely dissolved and the claret solution became yellow. Addition of $Na[S_2CNC_4H_8]\cdot nH_2O$ (80 mg, 0.38 mmol based on a 20% water content) gave a yellow precipitate. The mixture was extracted with CH_2Cl_2 and treated as for **1** to give $[Tc^{V}N(S_2CNC_4H_8)_2]$ (1.4 mg, 2.7%) and complex **2** (23.8 mg, 69% yield). Recrystallisation of **2** from CH_2Cl_2 gave yellow crystals, which start to darken and decompose at *ca.* 285 °C. Complex **2** is rather less soluble in CH_2Cl_2 than **1** and larger volumes were required for the extraction and chromatography (Found: Tc, 35.60. $C_{10}H_{16}N_4O_2S_4Tc_2$ requires Tc, 35.95%). IR: 1537vs, 1447m, 1442m, 1330m, 1157m, 1062s (Tc=N), 1055m (Tc≡N), 945m, 708m and 368m cm^{-1}. UV/VIS: λ_{max}/nm *ca.* 316(sh).

The IR spectrum of the $[TcN(S_2CNC_4H_8)_2]$ prepared above was identical with that of a sample prepared by the reaction of $[AsPh_4][TcNCl_4]$ in MeCN with $Na[S_2CNC_4H_8]$ (Found: Tc, 24.20. $C_{10}H_{16}N_3S_4Tc$ requires Tc, 24.40%).

$[AsPh_4][TcN(S_2CNEt_2)(SCOCOS)]$ **3**. Complex **1** (15 mg, 0.027 mmol) was dissolved in $SOCl_2$ (1 cm^3) and the purple solution taken to dryness on a rotary evaporator. The residue was dissolved in MeCN and $K_2[SCOCOS]$ (20 mg, 0.1 mmol), dissolved in water, was added followed by $AsPh_4Cl$ (15 mg, 0.036 mmol). The solution was taken to dryness, the complex

* *Supplementary data available:* see Instructions for Authors, *J. Chem. Soc., Dalton Trans.*, 1992, Issue 1, pp. xx–xxv.

Table 1 Crystallographic data and details of intensity data collection and structure refinement for $[\{TcN(S_2CNEt_2)\}_2(\mu\text{-}O)_2]$ **1** $[\{TcN(S_2CNC_4H_8)\}_2(\mu\text{-}O)_2]$ **2** and $[AsPh_4][TcN(S_2CNEt_2)(SCOCOS)]$ **3**

	1	**2**	**3**
Formula	$C_{10}H_{20}N_4O_2S_4Tc_2$	$C_{10}H_{16}N_4O_2S_4Tc_2$	$C_{31}H_{30}AsN_2O_2S_4Tc$
M	554.35	550.31	764.66
Crystal dimensions/mm	0.30 × 0.13 × 0.17	0.24 × 0.09 × 0.09	0.72 × 0.12 × 0.10
Colour	Yellow	Yellow	Red-brown
Crystal system	Triclinic	Monoclinic	Monoclinic
Space group	$P\bar{1}$	$P2_1/n$	$P2_1/n$
a/Å	8.069(2)	6.258(1)	20.670(10)
b/Å	9.224(2)	8.520(2)	15.740(6)
c/Å	14.017(3)	33.651(4)	10.162(5)
α/°	107.77(2)	90	90
β/°	102.05(2)	91.08(1)	93.61(4)
γ/°	93.80(2)	90	90
U/Å^3	962.1	1793.89	3299.61
Z	2	4	4
D_c/g cm^{-3}	1.91	2.04	1.54
$F(000)$	548	1080	1544
μ(Cu-Kα)/cm^{-1}	152.7	163.79	69.62
Transmission factors	0.085–0.3	0.176–0.365	0.200–0.560
Wavelength/Å	1.5418	1.5418	1.5418
$2\theta_{max}$/°	142	142	142
Data collected	Hemisphere	Quadrant	Quadrant
Scan rate/° min^{-1}	10	10	10
Scan range/°	1.4 + 0.4 tanθ	1.2 + 0.2 tanθ	1.3 + 0.3 tanθ
Independent data measured	3995	2871	5578
No. of unique data	3713	2871	5578
Rejection criterion $[I < n\sigma(I)]$	2	3	3
Terms used for refinement, N_o	3117	1817	3595
No. parameters refined, N_v	214	200	379
Weighting parameter, m $[w = (\sigma^2\|F_o\| + m\|F_o\|^2)^{-1}]$	0.0004	0.001	0.0015
R	0.028	0.075	0.094
R'	0.035	0.087	0.145
χ	1.24	1.72	2.75
Residual density/e Å^{-3}	+0.82, −0.48	+2.11, −2.13	+1.94, −2.4
Maximum Δ/σ for last cycle	0.03	0.01	0.04

extracted with water and the residue recrystallised from ethanol to give red-brown crystals, m.p. 191–192 °C (Found: Tc, 12.70. $C_{31}H_{30}AsN_2O_2S_4Tc$ requires Tc, 12.95%). IR: 1633vs, 1577m, 1523s, 1439s, 1283m, 1204m, 1079m, 1071s (Tc≡N), 1036s, 996m, 905m, 754m, 774s, 737s, 686s, 478m, 468s, 376m, 367m, 352m and 339m cm^{-1}. UV/VIS: λ_{max}/nm 289(sh) (ε/dm^3 mol^{-1} cm^{-1} 10 500) and 497 (200).

$[AsPh_4]_2[\{TcN(CN)_2\}_2(\mu\text{-}O)_2]$ **4**. To a solution of $Cs_2[TcNCl_5]$ (71 mg, 0.128 mmol) in saturated aqueous $Na_4P_2O_7{\cdot}10H_2O$ (3 cm^3) was added KCN (100 mg, 1.5 mmol) in water (1 cm^3). The bright yellow solution was filtered and $AsPh_4Cl$ (70 mg in 1 cm^3 of water) added to the filtrate to give a yellow precipitate which was collected by filtration, washed with water, and dried (decomposition commences at *ca.* 185 °C). Yield 62 mg, 86% (Found: C, 55.30; H, 3.45; N, 7.40; O, 3.00; Tc, 17.35. $C_{52}H_{40}As_2N_6O_2Tc_2$ requires C, 55.35; H, 3.55; N, 7.45; O, 2.85; Tc, 17.50%). IR: 3083m, 3060m, 1481s, 1438vs, 1338m, 1311m, 1185m, 1081s, 1069s (Tc≡N), 1062s (Tc≡N), 1022m, 997s, 748vs, 739vs, 723s, 689s, 477vs, 464vs, 459s, 421m, 404m, 385m, 360s, 348s, 328m and 262w cm^{-1}. UV/VIS: λ_{max}/nm 259 (ε/dm^3 mol^{-1} cm^{-1} 7960), 264 (8620), 271 (6830) and 341 (4040).

$[AsPh_4]_2[\{TcN(edt)\}_2(\mu\text{-}O)_2]$ **5**. To a solution of $Cs_2[TcNCl_5]$ (71 mg, 0.128 mmol) in saturated aqueous $Na_4P_2O_7{\cdot}10H_2O$ (3 cm^3) was added $HSCH_2CH_2SH$ (H_2edt) (0.1 cm^3, 1.2 mmol) dissolved in ethanol (0.4 cm^3). The mixture immediately turned orange and was shaken vigorously to break up the globules of H_2edt. After the addition of water (3 cm^3) the mixture was extracted with CH_2Cl_2 to remove excess H_2edt. Addition of $AsPh_4Cl$ (70 mg in 1 cm^3 of water) gave a bright yellow precipitate which was collected by filtration, washed well with water and dried *in vacuo*. Yield 68 mg, 88%, m.p. 246–248 °C (Found: C, 50.30; H, 3.80; N, 2.10; O, 2.90; S, 10.55; Tc, 15.90. $C_{52}H_{48}As_2N_2O_2S_4Tc_2$ requires C, 51.65; H, 4.00; N, 2.30; O, 2.65; S, 10.60; Tc, 16.35%). IR: 2887m, 1479m, 1438vs, 1274m, 1080s, 1046vs (Tc≡N), 1034m (Tc≡N), 997s, 745vs, 688vs, 477s, 468vs and 349s cm^{-1}. UV/VIS: λ_{max}/nm *ca.* 325(sh) (ε/dm^3 mol^{-1} cm^{-1} 8500).

ESR Spectroscopy.—The ESR spectra were recorded at 130 K using a Bruker ESR-200D-SRC spectrometer and associated equipment. All solutions were 2 × 10^{-3} mol dm^{-3} in Tc. Spectral simulations were performed on a Data General MV8000 computer using the programs described previously.[8] The spin Hamiltonian was of the form shown below,

$$\mathcal{H} = g_{\parallel}\beta B_z S_z + g_{\perp}\beta(B_x S_x + B_y S_y) + A_{\parallel} S_z I_z + A_{\perp}(S_x I_x + S_y I_y) + Q[I^2_z - I(I+1)/3] + \mathcal{H}_{s.h.f.}$$

where $S = \frac{1}{2}$, $I = \frac{9}{2}$ for the Tc^{VI} ion and the other symbols have their usual meaning; $\mathcal{H}_{s.h.f.}$ is the ligand superhyperfine term, the general form of which has been described previously.[8]

X-Ray Crystallography.—Single crystals of $[\{TcN(S_2CNC_4H_8)\}_2(\mu\text{-}O)_2]$**2**and$[AsPh_4][TcN(S_2CNEt_2)(SCOCOS)]$ **3** suitable for X-ray diffraction studies were grown by slow evaporation of CH_2Cl_2 and EtOH solutions, respectively. Unit-cell parameters were obtained in each case by least-squares analyses[9] of the setting angles, determined on a diffractometer at 23 °C with Cu-Kα radiation, for 30 reflections well separated in reciprocal space.

Intensity data were recorded at 23 ± 1 °C on an automated Siemens AED diffractometer with nickel-filtered Cu-Kα

Table 2 Atomic coordinates (with e.s.d.s in parentheses) for [{TcN-(S_2CNEt_2)}$_2(\mu\text{-}O)_2$] **1**

Atom	*X/a*	*Y/b*	*Z/c*
Tc(1)	0.1248(1)	0.1107(1)	0.2774(1)
Tc(2)	0.2528(1)	0.2314(1)	0.1636(1)
O(1)	0.3474(4)	0.2279(3)	0.3020(2)
O(2)	0.0771(4)	0.0577(3)	0.1288(2)
S(1)	0.2618(2)	0.0204(1)	0.4163(1)
S(2)	−0.0200(2)	−0.1454(1)	0.2466(1)
S(3)	0.2746(1)	0.1287(1)	−0.0144(1)
S(4)	0.5469(1)	0.2982(1)	0.1596(1)
N(1)	−0.0065(6)	0.2228(4)	0.3235(3)
N(2)	0.1694(6)	0.3884(4)	0.1692(3)
N(3)	0.1107(5)	−0.2598(4)	0.3971(2)
N(4)	0.5897(5)	0.2165(4)	−0.0334(3)
C(1)	0.1152(5)	−0.1453(4)	0.3597(3)
C(2)	0.2401(7)	−0.2591(5)	0.4887(3)
C(3)	0.3829(8)	−0.3496(7)	0.4602(4)
C(4)	−0.0187(7)	−0.3972(5)	0.3469(3)
C(5)	−0.1685(8)	−0.3888(7)	0.3951(4)
C(6)	0.4856(5)	0.2153(4)	0.0271(3)
C(7)	0.5335(7)	0.1381(5)	−0.1461(3)
C(8)	0.5198(9)	0.2451(7)	−0.2086(4)
C(9)	0.7687(6)	0.2907(5)	0.0093(4)
C(10)	0.7863(8)	0.4635(6)	0.0317(4)

Table 3 Atomic coordinates (with e.s.d.s in parentheses) for [{TcN-$(S_2CNC_4H_8)$}$_2(\mu\text{-}O)_2$] **2**

Atom	*X/a*	*Y/b*	*Z/c*
Tc(1)	0.3090(3)	0.0651(2)	0.1569(1)
Tc(2)	0.3329(3)	0.2400(2)	0.0959(2)
S(1)	0.5890(11)	−0.0625(7)	0.1965(2)
S(2)	0.2498(9)	0.1280(7)	0.2265(2)
S(3)	0.6322(8)	0.3285(6)	0.0554(2)
S(4)	0.3089(8)	0.5252(6)	0.0900(2)
O(1)	0.185(2)	0.270(2)	0.145(1)
O(2)	0.525(2)	0.079(2)	0.117(1)
N(1)	0.138(3)	−0.075(2)	0.145(1)
N(2)	0.174(3)	0.170(2)	0.063(1)
N(3)	0.553(3)	0.005(2)	0.274(1)
N(4)	0.639(2)	0.642(2)	0.050(1)
C(1)	0.478(3)	0.018(2)	0.238(1)
C(2)	0.754(3)	−0.088(3)	0.282(1)
C(3)	0.777(4)	−0.079(4)	0.326(1)
C(4)	0.646(3)	0.064(3)	0.340(1)
C(5)	0.475(3)	0.080(2)	0.308(1)
C(6)	0.540(3)	0.518(2)	0.062(1)
C(7)	0.566(3)	0.802(2)	0.058(1)
C(8)	0.731(3)	0.910(2)	0.037(1)
C(9)	0.930(3)	0.803(2)	0.035(1)
C(10)	0.839(3)	0.637(2)	0.028(1)

radiation. Intensities were measured by a background-peak-background θ–2θ scan procedure. Crystal data and conditions for data collections are given in Table 1. The integrated intensities were corrected for Lorentz and polarisation effects and for absorption.[10]

Structure determinations and refinements. The sites of the Tc atoms of **2** and those of Tc and As (and most of the non-hydrogen atoms) of **3** were determined from an electron density map generated by the SHELXS 86 program system.[11] Subsequent difference syntheses using SHELX 76 revealed the sites of all the remaining non-hydrogen atoms for the two structures.[12] The hydrogen atoms of the methylene groups for **2** and **3** and those of the $[AsPh_4]^+$ cation for **3** were included in the analysis at calculated positions, whereas those of the methyl carbons for **3** were set up as staggered methyl groups and then refined as rigid groups. The hydrogen atoms were assigned common overall isotropic thermal parameters.

The structures were refined by the full-matrix least-squares method, with anisotropic thermal parameters given to non-hydrogen atoms. The *R* indices are defined as $R = \Sigma\Delta F/\Sigma|F_o|$, $R' = [\Sigma w(\Delta F)^2/\Sigma wF_o^2]^{\frac{1}{2}}$, and the 'goodness of fit', χ, as

Table 4 Atomic coordinates (with e.s.d.s in parentheses) for $[AsPh_4]$-[TcN(S_2CNEt_2)(SCOCOS)] **3**

Atom	*X/a*	*Y/b*	*Z/c*
Tc	0.1630(1)	0.2044(1)	0.0506(1)
As	−0.0403(1)	0.3872(1)	0.7098(2)
S(4)	0.2007(3)	0.1496(3)	0.2617(5)
S(2)	0.1511(3)	0.1884(4)	−0.1820(5)
S(3)	0.1075(3)	0.0707(3)	0.0802(5)
S(1)	0.2649(3)	0.2690(3)	0.0207(6)
N(1)	0.116(1)	0.276(1)	0.085(2)
N(2)	0.141(1)	0.000(1)	0.316(2)
O(1)	0.310(1)	0.325(2)	−0.192(2)
O(2)	0.216(1)	0.263(2)	−0.361(2)
C(1)	0.264(2)	0.287(2)	−0.150(3)
C(2)	0.213(1)	0.245(2)	−0.244(3)
C(3)	0.148(1)	0.064(1)	0.232(2)
C(4)	0.180(1)	−0.002(2)	0.444(3)
C(5)	0.146(2)	0.032(2)	0.550(3)
C(6)	0.097(1)	−0.069(1)	0.286(3)
C(7)	0.027(1)	−0.053(2)	0.314(3)
C(8)	−0.073(1)	0.310(1)	0.838(2)
C(9)	−0.136(1)	0.308(1)	0.859(2)
C(10)	−0.160(1)	0.251(1)	0.949(2)
C(11)	−0.115(1)	0.197(1)	1.022(2)
C(12)	−0.051(1)	0.198(1)	0.998(2)
C(13)	−0.026(1)	0.255(1)	0.905(2)
C(14)	0.032(1)	0.457(1)	0.780(2)
C(15)	0.087(1)	0.417(1)	0.836(2)
C(16)	0.139(1)	0.466(2)	0.876(2)
C(17)	0.138(1)	0.554(1)	0.864(2)
C(18)	0.081(1)	0.592(1)	0.811(2)
C(19)	0.027(1)	0.545(1)	0.767(2)
C(20)	−0.009(1)	0.323(1)	0.569(2)
C(21)	0.053(1)	0.329(1)	0.527(2)
C(22)	0.073(1)	0.280(1)	0.427(2)
C(23)	0.027(1)	0.222(1)	0.359(2)
C(24)	−0.034(1)	0.215(1)	0.403(2)
C(25)	−0.052(1)	0.264(1)	0.508(2)
C(26)	−0.112(1)	0.460(1)	0.652(2)
C(27)	−0.142(1)	0.451(1)	0.526(2)
C(28)	−0.195(1)	0.501(2)	0.492(2)
C(29)	−0.220(1)	0.557(1)	0.578(3)
C(30)	−0.189(1)	0.565(1)	0.702(3)
C(31)	−0.139(1)	0.515(1)	0.739(2)

Table 5 Selected bond lengths (Å) and angles (°) for [{TcN(S_2-$CNEt_2$)}$_2(\mu\text{-}O)_2$] **1**

Tc(1)–Tc(2)	2.543(1)		
Tc(1)–N(1)	1.623(4)	Tc(2)–N(2)	1.624(4)
Tc(1)–O(1)	1.942(3)	Tc(2)–O(1)	1.942(3)
Tc(1)–O(2)	1.935(3)	Tc(2)–O(2)	1.936(3)
Tc(1)–S(1)	2.433(1)	Tc(2)–S(3)	2.433(1)
Tc(1)–S(2)	2.436(1)	Tc(2)–S(4)	2.428(1)
S(1)–C(1)	1.730(4)	S(3)–C(6)	1.731(4)
S(2)–C(1)	1.726(4)	S(4)–C(6)	1.726(4)
N(3)–C(1)	1.317(5)	N(4)–C(6)	1.313(5)
N(3)–C(2)	1.474(5)	N(4)–C(7)	1.478(5)
N(3)–C(4)	1.471(5)	N(4)–C(9)	1.474(6)
C(2)–C(3)	1.517(7)	C(7)–C(8)	1.501(6)
C(4)–C(5)	1.498(7)	C(9)–C(10)	1.518(7)
Tc(1)–O(1)–Tc(2)	81.8(1)	Tc(1)–O(2)–Tc(2)	82.1(1)
O(1)–Tc(1)–O(2)	94.7(1)	O(1)–Tc(2)–O(2)	94.6(1)
N(1)–Tc(1)–S(1)	105.8(1)	N(2)–Tc(2)–S(3)	104.2(1)
N(1)–Tc(1)–S(2)	103.2(2)	N(2)–Tc(2)–S(4)	103.9(2)
N(1)–Tc(1)–O(1)	110.4(2)	N(2)–Tc(2)–O(1)	110.0(2)
N(1)–Tc(1)–O(2)	110.7(2)	N(2)–Tc(2)–O(2)	111.1(2)
S(1)–Tc(1)–S(2)	72.2(1)	S(3)–Tc(2)–S(4)	72.2(1)

Table 6 Selected bond lengths (Å) and angles (°) for [{TcN(S$_2$CNC$_4$H$_8$)}$_2$(μ-O)$_2$] **2**

Tc(1)–Tc(2)	2.542(2)		
Tc(1)–N(1)	1.65(2)	Tc(2)–N(2)	1.59(2)
Tc(1)–S(1)	2.437(6)	Tc(2)–S(3)	2.457(5)
Tc(1)–S(2)	2.439(5)	Tc(2)–S(4)	2.442(5)
Tc(1)–O(1)	1.947(12)	Tc(2)–O(1)	1.934(13)
Tc(1)–O(2)	1.936(12)	Tc(2)–O(2)	1.943(13)
C(1)–S(1)	1.71(2)	C(6)–S(3)	1.73(2)
C(1)–S(2)	1.75(2)	C(6)–S(4)	1.74(2)
C(1)–N(3)	1.28(2)	C(6)–N(4)	1.30(2)
C(2)–N(3)	1.51(2)	C(7)–N(4)	1.47(2)
C(2)–C(3)	1.49(3)	C(7)–C(8)	1.56(2)
C(3)–C(4)	1.55(3)	C(8)–C(9)	1.55(2)
C(4)–C(5)	1.50(3)	C(9)–C(10)	1.54(3)
C(5)–N(3)	1.43(2)	C(10)–N(4)	1.47(2)
Tc(1)–O(1)–Tc(2)	81.8(5)	Tc(1)–O(2)–Tc(2)	81.9(5)
O(1)–Tc(1)–O(2)	94.9(5)	O(1)–Tc(2)–O(2)	95.1(5)
N(1)–Tc(1)–S(1)	105.5(8)	N(2)–Tc(2)–S(3)	101.8(6)
N(1)–Tc(1)–S(2)	106.4(7)	N(2)–Tc(2)–S(4)	106.2(7)
N(1)–Tc(1)–O(1)	110.3(8)	N(2)–Tc(2)–O(1)	110.1(7)
N(1)–Tc(1)–O(2)	109.6(8)	N(2)–Tc(2)–O(2)	111.2(8)
S(1)–Tc(1)–S(2)	72.1(2)	S(3)–Tc(2)–S(4)	72.3(2)

Table 7 Selected bond lengths (Å) and angles (°) for [AsPh$_4$][TcN(S$_2$CNEt$_2$)(SCOCOS)] **3**

Tc–N(1)	1.54(2)	Tc–S(1)	2.377(5)
Tc–S(2)	2.374(6)	Tc–S(3)	2.424(5)
Tc–S(4)	2.396(5)	S(1)–C(1)	1.76(3)
S(2)–C(2)	1.72(3)	S(3)–C(3)	1.72(2)
S(4)–C(3)	1.74(2)	C(1)–C(2)	1.53(4)
C(1)–O(1)	1.22(3)	C(2)–O(2)	1.23(3)
C(3)–N(2)	1.34(2)	C(4)–N(2)	1.49(3)
C(4)–C(5)	1.44(3)	C(6)–N(2)	1.45(3)
C(6)–C(7)	1.51(3)	As–C(8)	1.93(2)
As–C(14)	1.94(2)	As–C(20)	1.90(2)
As–C(26)	1.94(1)		
N(1)–Tc–S(1)	107.3(6)	N(1)–Tc–S(2)	105.9(6)
N(1)–Tc–S(3)	107.0(6)	N(1)–Tc–S(4)	103.7(6)
S(1)–Tc–S(2)	87.4(2)	S(1)–Tc–S(4)	91.6(2)
S(2)–Tc–S(3)	90.7(2)	S(3)–Tc–S(4)	72.9(2)
C(8)–As–C(14)	113.3(8)	C(8)–As–C(20)	108.8(7)
C(8)–As–C(26)	106.7(8)	C(14)–As–C(20)	106.5(8)
C(14)–As–C(26)	109.6(8)	C(20)–As–C(26)	111.9(7)

$[\Sigma w(\Delta F)^2/(N_o - N_v)]^{\frac{1}{2}}$ where $\Delta F = ||F_o| - |F_c||$, N_o is the number of reflections used in the refinement, and N_v is the number of variables. The function minimised was $\Sigma w(\Delta F)^2$. An empirical isotropic extinction correction was refined. Refinement indices are given in Table 1.

During the refinement of **2**, based on 1817 non-zero data, it was observed that 23 of the weakest intensity reflections exhibited relatively poor agreement with the calculated structure factors, and in all cases $F_o \gg F_c$ and the k indices were restricted to the values of 9 and 10. As this effect was clearly systematic, it was decided to omit these low-intensity data from further refinement cycles.

Neutral atom scattering-factor curves for carbon, nitrogen, oxygen and chlorine were taken from ref. 13, those for technetium and arsenic were from ref. 14, and that for hydrogen was from ref. 15. Real and imaginary anomalous dispersion corrections were applied to the non-hydrogen atoms.[10] Figs. 3, 4 and 6 have been prepared from the output of ORTEP.[16] Fractional coordinates for [{TcN(S$_2$CNEt$_2$)}$_2$(μ-O)$_2$] **1**, [{TcN(S$_2$CNC$_4$H$_8$)}$_2$(μ-O)$_2$] **2** and [AsPh$_4$][TcN(S$_2$CNEt$_2$)(SCOCOS)] **3** are given in Tables 2–4, respectively and selected interatomic bond lengths and angles in Tables 5–7, respectively.

Additional material available from the Cambridge Crystallographic Data Centre comprises thermal parameters and remaining bond lengths and angles.

Results and Discussion

The complexes R[Tc^{VI}NX$_4$] (R = AsPh$_4$ or NBu$_4$, X = Cl or Br) dissolved in organic solvents such as MeCN have been shown to undergo substitution reactions readily with a variety of ligands to give monomeric products, generally with concomitant reduction to Tc^{V}N.[7,17,18] Reduction has been found to occur even upon substitution by non-reducing ligands such as 2,2′-bipyridyl[19] or 1,10-phenanthroline.[20] The reaction of [AsPh$_4$][TcNCl$_4$] in acetone with aqueous oxalic acid, however, gave red-brown crystals of the cyclic tetramer [AsPh$_4$]$_4$[Tc$_4$N$_4$O$_2$(ox)$_6$] which has been shown by X-ray crystallography to consist of two (ox)NTc^{VI}–O–Tc^{VI}N(ox) dimeric units joined by two quadridentate oxalato ligands.[6] We have since shown that Cs$_2$[TcNCl$_5$] is hydrolysed to give a brown precipitate of 'TcN(OH)$_3$' which has been formulated as the dimer [{TcN(OH)(OH$_2$)}$_2$(μ-O)$_2$] (or alternatively as the polymers [{TcN(OH)(OH$_2$)(μ-O)}$_n$] or [{TcN(OH)(μ-O)}$_n$]·nH$_2$O).[4,8] This precipitate dissolves in solutions of non-coordinating acids, such as toluene-*p*-sulfonic acid, to give the aquanitrido cation [{TcN(OH$_2$)$_3$}$_2$(μ-O)$_2$]$^{2+}$. Reaction of the aqua cation with Na[S$_2$CNEt$_2$] gives the di-μ-oxo dimer [{TcN(S$_2$CNEt$_2$)}$_2$(μ-O)$_2$] **1** in 37% yield together with 15% of [Tc^{V}N(S$_2$CNEt$_2$)$_2$].[5] Better yields of **1** may be obtained by the reaction of Na[S$_2$CNEt$_2$] with Cs$_2$[TcNCl$_5$] dissolved in NaOH or Na$_4$P$_2$O$_7$ solution.[4] The pyrrolidinyl derivative [{TcN(S$_2$CNC$_4$H$_8$)}$_2$(μ-O)$_2$] **2** has been prepared in Na$_4$P$_2$O$_7$ solution in 69% yield together with only *ca.* 3% of the reduced species [TcN(S$_2$CNC$_4$H$_8$)$_2$]. The reaction of R[TcNX$_4$] with dithiocarbamates in organic solvents has previously resulted only in the isolation of the [TcN(S$_2$CNR$_2$)$_2$] complexes.[7]

The IR spectra of complexes **1** and **2** show the two ν(Tc≡N) absorptions expected on the basis of the *syn* (non-centrosymmetric) stereochemistry. For **1** these absorptions occur at 1061 and 1054 cm^{-1} with the absorption at the higher wavenumber being the more intense as is the case for the ν(Mo=O) absorptions in [{MoO(S$_2$CNEt$_2$)}$_2$(μ-O)$_2$] (973 and 956 cm^{-1}).[21] The IR spectra of a range of mono- and di-meric Mo^{V}O 1,1-dithiolate complexes have been studied by Chen *et al.*[21] by the use of ^{18}O labelling. These authors found that in [MoO(L–L)$_2$] (L–L = a 1,1-dithiolate), ν(Mo=O) absorption occurs at 965 ± 8 cm^{-1} and in [Mo$_2$O$_4$(L–L)$_2$] ν(Mo=O) is centred at 975 ± 6 cm^{-1}. The TcN analogues appear to show the reverse trend with ν(Tc≡N) at 1070 cm^{-1} for [TcN(S$_2$CNEt$_2$)$_2$][22] and ν(Tc≡N) centred at 1058 ± 1 cm^{-1} for complexes **1** and **2**. Peaks at 704 and 708 cm^{-1} for **1** and **2**, respectively, are assigned to ν$_{asym}$(Tc–O–Tc) and correlate well with the corresponding ν$_{asym}$(Mo–O–Mo) at 730 cm^{-1} for [{MoO(S$_2$CNEt$_2$)}$_2$(μ-O)$_2$].[21]

Dissolution of complex **1** in SOCl$_2$ gave a deep blue solution which is shown by ESR spectroscopy (see later) to contain [Tc^{VI}NCl$_2$(S$_2$CNEt$_2$)]. Removal of the solvent and reaction with K$_2$[SCOCOS] gave the Tc^{V}N mixed-ligand complex [AsPh$_4$][TcN(S$_2$CNEt$_2$)(SCOCOS)] **3**. The IR spectrum of this complex showed a single intense ν(Tc≡N) absorption at 1071 cm^{-1} and a mixture of ligand peaks which resembled the sum of the spectra of [TcN(S$_2$CNEt$_2$)$_2$][22] and [AsPh$_4$]$_2$[TcN(SCOCOS)$_2$].[18a]

The ν(C–N) absorptions occur at 1512 cm^{-1} for [TcN(S$_2$CNEt$_2$)$_2$] and at 1532 and 1537 cm^{-1} for complexes **1** and **2**, respectively, indicating the greater contribution of resonance form **B** in **1** and **2**. This difference may be due in part to the

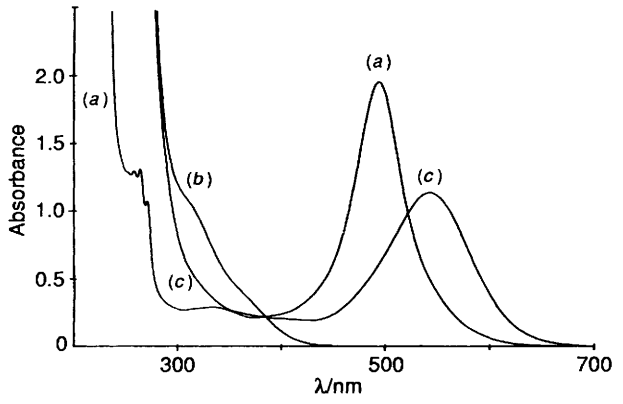

Fig. 1 UV/VIS spectra in MeCN solution of (*a*) 5×10^{-5} mol dm^{-3} $[AsPh_4]_4[Tc_4N_4O_2(ox)_6]$, (*b*) 1×10^{-4} mol dm^{-3} **1** and (*c*) 1×10^{-4} mol dm^{-3} **1** to which two equivalents of solid $AsPh_4Cl{\cdot}HCl$ have been added

oxidation state of +6 for technetium in the dimers, but the presence of the bridging oxygen atoms is probably more important since in $[Tc^{VI}NCl_2(S_2CNEt_2)]$, which contains two chloro ligands, ν(C–N) occurs at 1550 cm^{-1}.

Reaction of $Cs_2[TcNCl_5]$–$Na_4P_2O_7$ with cyanide gave $[AsPh_4]_2[\{TcN(CN)_2\}_2(\mu\text{-}O)_2]$ **4** in good yield. This formulation is based on the microanalytical data (in particular, the presence of one oxygen atom per technetium has been established) and the IR spectrum, which shows two ν(Tc≡N) absorptions of approximately equal intensity at 1069 and 1062 cm^{-1} and ν_{asym}(Tc–O–Tc) at 723 cm^{-1}. A puzzling feature is the presence of only a very weak peak at 2157 cm^{-1} which can be assigned to ν(C≡N). However, when a solution of **4** in MeCN was treated with '$AsPh_4Cl{\cdot}HCl$' [structure $(AsPh_4)(H_5O_2)Cl_2$,[23] a convenient reagent for the addition of small amounts of HCl in organic solvents] the purple product (λ_{max} 535 nm) showed an intense ν(C≡N) at 2155 cm^{-1}. We have previously reported that dissolution of $Cs_2[TcNCl_5]$ in aqueous KCN gave a yellow solution which showed no ESR signals and from which the structurally characterised $[AsPh_4]_2[Tc^{V}N(CN)_4(OH_2)]$ was isolated in 63% yield.[17] Treatment of the yellow solution with concentrated HCl gave an intense purple colour which turned orange on heating and $[AsPh_4][TcNCl_4]$ was isolated in 30% yield. It is now clear that the formation of $[TcNCl_4]^-$, which was interpreted as arising from the oxidation of Tc^{V} to Tc^{VI},[17] is due to the cleavage of the technetium(VI) dimeric complex {present together with the reduced species $[Tc^{V}N(CN)_4(OH_2)]^{2-}$} to $[TcN(CN)_2Cl_2]^-$ followed by stepwise substitution of CN^- by Cl^-.

Reaction of $Cs_2[TcNCl_5]$–$Na_4P_2O_7$ with ethane-1,2-dithiol gave a yellow product which showed an intense ν(Tc≡N) peak at 1046 cm^{-1} and a weaker peak at 1034 cm^{-1} and analysed as slightly impure $[AsPh_4]_2[\{TcN(edt)\}_2(\mu\text{-}O)_2]$ **5**. The microanalysis established the presence of one oxygen atom per technetium, but the ν_{asym}(Tc–O–Tc) absorption could not be identified, possibly due to superimposition by the intense absorptions arising from the phenyl rings of $[AsPh_4]^+$. Similarly Dance *et al.*[24] could not identify the bridging oxygen vibrations in a series of complexes $[NR_4]_2[Mo_2O_4L_4]$ (R = Me or Et; L = SPh or $\frac{1}{2}SCH_2CH_2CH_2S$). We have previously reported that the reaction of benzene-1,2-dithiol (H_2bdt) with $[AsPh_4][TcNCl_4]$ in acetone results in the loss of the nitrido ligand and the formation of the trigonal-prismatic complex $[AsPh_4][Tc(bdt)_3]$.[25] The same reaction with ethane-1,2-dithiol in organic solvents gave an insoluble and intractable green-black product.

The nature of the species in the $Cs_2[TcNCl_5]$–$Na_4P_2O_7$ solution is unknown, but the Tc^{VI} state is clearly retained. The absence of ESR signals indicates the formation of either a diamagnetic di-μ-oxo dimer or a polymer.[4] Reaction of this solution with a variety of ligands has been shown to be a convenient method for the preparation of complexes containing the $[NTc^{VI}(\mu\text{-}O)_2Tc^{VI}N]^{2+}$ core.

Comparison of $Tc^{VI}N$ *and* $Mo^{V}O$ *Chemistries.*—The formation of oxo-bridged nitrido complexes appears to be unique to technetium and since $Tc^{VI}N$ is isoelectronic with $Mo^{V}O$, similarities in the chemistries of these two systems may be expected. A large number of dimeric complexes based on $[Mo_2O_3]^{4+}$ and $[Mo_2O_4]^{2+}$ cores have been prepared and intensively studied,[1–3] and provide a guide and scope for comparison with the chemistry of complexes based on the $[Tc_2N_2O]^{4+}$ and $[Tc_2N_2O_2]^{2+}$ cores. This comparison may be extended to the isoelectronic $Tc^{VII}N$ and $Mo^{VI}O$ where the preparation of novel peroxonitrido complexes such as $[AsPh_4][TcN(O_2)_2X]$ (X = Cl or Br) and $[TcN(O_2)_2(L\text{–}L)]$ (L–L = 2,2′-bipyridyl or 1,10-phenanthroline), which are analogues of the well known $[MoO(O_2)_2]$ complexes, has been reported recently.[26] However, differences in the stability of $Tc^{VI}N$ and $Mo^{V}O$ to oxidation and the greater π-donation ability of the nitrido (N^{3-}) compared to the oxo (O^{2-}) ligand result in different chemical behaviour. Thus, while TcN complexes are known in the +7, +6 and +5 oxidation states and MoO complexes in the +6, +5 and +4 oxidation states, the $Tc^{VI}N$ and $Tc^{V}N$ species are difficult to oxidise while the corresponding $Mo^{V}O$ and $Mo^{IV}O$ species are readily oxidised.[1]

A characteristic reaction in molybdenum chemistry is the comproportionation equilibrium (1).[27,28] When L_2 is $Et_2NCS_2^-$,

$$Mo^{IV}OL_4 + Mo^{VI}O_2L_4 \rightleftharpoons \underset{\mathbf{6}}{L_4OMo^{V}\text{–}O\text{–}Mo^{V}OL_4} \quad (1)$$

the μ-oxo complex **6** shows an intense visible absorption at 510 nm.[28] Intense absorptions at *ca.* 525 nm are considered to be characteristic of linear (or near-linear) Mo^{V}–O–Mo^{V} complexes,[1] but this absorption appears to be somewhat ligand dependent and occurs at 462 nm in $[\{MoOCl[HB(pz)_3]\}_2(\mu\text{-}O)]$ [$HB(pz)_3$ = hydrotris(pyrazol-1-yl)borate].[29]

A spectrophotometric study showed no evidence for reaction (2), which is the isoelectronic equivalent of equation (1). In this

$$[Tc^{V}N(S_2CNEt_2)_2] + [Mo^{VI}O_2(S_2CNEt_2)_2] \not\rightarrow [(Et_2NCS_2)_2NTc^{VI}(\mu\text{-}O)Mo^{V}O(S_2CNEt_2)_2] \quad (2)$$

study the concentration of $[TcN(S_2CNEt_2)_2]$ was varied from 6.25×10^{-4} to 0.01 mol dm^{-3} in MeCN in the presence of four equivalents of $[MoO_2(S_2CNEt_2)_2]$. Addition of PPh_3 to the solution produced the expected intense purple colour due to $[Mo_2O_3(S_2CNEt_2)_4]$ (λ_{max} = 511 nm). The absence of reaction (2) is not surprising in view of the difficulty in oxidising $Tc^{V}N$ to $Tc^{VI}N$. The only fully characterised NTc^{VI}–O–$Tc^{VI}N$ complex is $[AsPh_4]_4[Tc_4N_4O_2(ox)_6]$, the electronic spectrum of which (previously unreported) shows an intense absorption at 493 nm (ε = 39 200 dm^3 mol^{-1} cm^{-1}) [Fig. 1(*a*)]. The UV spectrum of complex **1** shows only a shoulder at *ca.* 316 nm [Fig. 1(*b*)]. Addition of two equivalents of $AsPh_4Cl{\cdot}HCl$ to a MeCN solution of **1** produced an intense purple colour (λ_{max} 545 nm) [Fig. 1(*c*)] which is ascribed to the formation of the μ-oxo dimer **7** [equation (3)]. For complex **2** the purple colour resulted in λ_{max} 544 nm.

$$[Tc_2N_2O_2(S_2CNEt_2)_2] + 2AsPh_4Cl{\cdot}HCl \longrightarrow \underset{\mathbf{7}}{[AsPh_4]_2[(Et_2NCS_2)Cl_2NTc(\mu\text{-}O)TcNCl_2(S_2CNEt_2)]} + H_2O \quad (3)$$

ESR Spectra.—The ESR spectrum of complex **1** in $SOCl_2$ when frozen to 130 K was well resolved and is shown in part in Fig. 2. The parallel components of the spectrum show evidence for the presence of two similar species, as is observed, for example, in solutions of $[AsPh_4][TcNCl_4]$ in $SOCl_2$.[30] The perpendicular features show clear evidence for superhyperfine interactions. The spectrum was best fitted by simulations which incorporate the superhyperfine interactions arising from two

Table 8 ESR spectral parameters of $Tc^{VI}N$ monomeric complexes. All hyperfine, superhyperfine and quadrupole interaction parameters are given in units of $\times 10^4$ cm^{-1}

System	$g_{\parallel}$ (± 0.001)	$g_{\perp}$ (± 0.002)	$A_{\parallel}$ (± 0.3)	$A_{\perp}$ (± 0.5)	Q (± 1.0)	a_x	a_y (± 2.0)	a_z
$[TcNCl_2(S_2CNEt_2)]$	2.016	2.002	268.0	123.0	3.0	11	14	1
$[TcNCl_2(S_2CNC_4H_8)]$	2.014	2.002	269.0	125.0	2.5	See text		
$[TcNCl_2(CN)_2]^-$	2.014	2.005	258.7	113.0	3.5	See text		

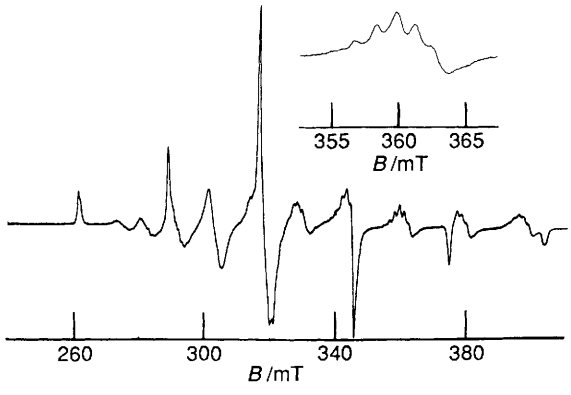

Fig. 2 ESR spectrum of $[\{TcN(S_2CNEt_2)\}_2(\mu\text{-}O)_2]$ **1** (2.0×10^{-3} mol dm^{-3}) in $SOCl_2$ at 130 K. Spectrometer settings: gain 4.0×10^4, 100 kHz modulation amplitude 0.5 mT, microwave power 2 mW, microwave frequency 9.522 GHz. The outermost parallel features at *ca.* 208, 235, 434 and 465 mT are not shown. The inset shows an expansion of one of the perpendicular features of the spectrum (gain 6.3×10^4, 100 kHz modulation amplitude 0.2 mT, microwave power 20 mW)

nuclei with $I = \frac{3}{2}$ located in the plane perpendicular to the Tc≡N direction and *cis* to each other. The spin Hamiltonian parameters are given in Table 8. Since the chlorine nucleus has $I = \frac{3}{2}$, the species in solution is identified as $[TcNCl_2(S_2CNEt_2)]$, resulting from the cleavage of the di-μ-oxo bridge of complex **1** and substitution of oxygen by chlorine. Since ^{32}S has no nuclear spin it cannot contribute to the superhyperfine interaction. Whilst the simulations were able to reproduce the overall shape of the spectrum, there were discrepancies in detail between the field positions of observed and simulated spectra. These indicate that the model used, which assumed coincidence of the *g* values, technetium hyperfine and chloride ligand superhyperfine tensor axes, is inadequate. This is not surprising in view of the low symmetry of the $[TcNCl_2(S_2CNEt_2)]$ molecule. The ESR spectra of some molecules of similarly low symmetry, where the *g* and hyperfine tensor axes are non-coincident, have been reported by Scullane *et al.*[31] and Collison *et al.*[32]

A similar, but less well resolved spectrum was observed for solutions of complex **2** in $SOCl_2$. The overall width of the perpendicular features could be simulated using the same magnitude chloride s.h.f. interaction as for the solutions of complex **1**. For solutions left to stand for 20 min prior to freezing, there was evidence for the development of a broad resonance, which is probably due to solute aggregation.

The cleavage of the dimeric complex $[AsPh_4]_2[\{TcN(CN)_2\}_2(\mu\text{-}O)_2]$ **4** in solution was studied. No ESR signals were observed from a solution of this complex in $SOCl_2$ when frozen immediately after addition of $SOCl_2$. The solution was claret-orange and the absence of ESR signals indicated that cleavage of one oxygen bridge had occurred to give the singly bridged dimer, which is expected to be diamagnetic. The ESR signals which developed after heating could be correlated with species previously identified as $[TcNCl_2(CN)_2]^-$, $[TcNCl_3(CN)]^-$ and $[TcNCl_4]^-$.[17] The most prominent species was that associated with $[TcNCl_3(CN)]^-$, but the signals associated with $[TcNCl_4]^-$ became relatively stronger and increased in absolute intensity after further warming.

A controlled cleavage of **4** could be achieved in MeCN solution by the addition of $AsPh_4Cl$·HCl, two equivalents of which gave a purple solution (λ_{max} 534 nm) which exhibited no ESR signals, even on heating. Addition of four equivalents resulted in a deeper purple colour and the weak ESR signals previously attributed to $[TcNCl_2(CN)_2]^-$.[17] When twelve equivalents of $AsPh_4Cl$·HCl were added the solution was orange and exhibited strong ESR signals due to this species. The best resolved spectrum was obtained when a few drops of concentrated HCl were added to the MeCN solution to which two equivalents of $AsPh_4Cl$·HCl had previously been added. The spectrum showed the presence of only one ESR active species, and the partial resolution of superhyperfine structure in the perpendicular direction established the co-ordination of two chloride ions. The chloride s.h.f. interaction appeared to be similar to that found for $[TcNCl_2(S_2CNEt_2)]$. The spin Hamiltonian parameters are listed in Table 8.

Structural Studies.—$[\{TcN(S_2CNEt_2)\}_2(\mu\text{-}O)_2]$ **1** and $[\{TcN(S_2CNC_4H_8)\}_2(\mu\text{-}O)_2]$ **2**. The structures of complexes **1** and **2** consist of discrete dimeric units of $[\{TcN(S_2CNR_2)\}_2(\mu\text{-}O)_2]$ (R = Et **1** or $R_2 = C_4H_8$ **2**). Perspective views of **1** and **2**, which include the atom numbering, are shown in Figs. 3 and 4, respectively. Complex **1** is isostructural with the oxomolybdenum analogue $[\{MoO(S_2CNEt_2)\}_2(\mu\text{-}O)_2]$.[33] The co-ordination geometry about the Tc atoms in **1** and **2** is distorted square-pyramidal with the two square pyramids in each complex fused at an edge containing the bridging oxygen atoms. Both complexes are *syn* isomers, with dihedral angles of 150.8(3) and 151.5(3)° for **1** and **2** respectively, between the planes formed by the technetium atom and the bridging oxygen atoms of each pyramid. This bending between pyramids is clearly illustrated in Fig. 5, which shows a side view of **1**. The Tc atoms are displaced above the corresponding S_2O_2 basal planes by 0.65(1) Å for **1** and by 0.67(1) and 0.65(1) Å for **2**. These values are similar to those observed in other five-co-ordinate complexes of technetium.[34]

The Tc–Tc distances of 2.543(1) and 2.542(2) Å for complexes **1** and **2** respectively are shorter than that of 2.580(1) Å for the Mo–Mo bond reported in the complex $[\{MoO(S_2CNEt_2)\}_2(\mu\text{-}O)_2]$. The acute Tc–O–Tc angles and the relatively short Tc–Tc distances indicate the presence of a metal–metal single bond, which is consistent with the results of molecular orbital calculations for molybdenum systems[35] and the absence of ESR signals from **1** and **2**. The Tc–Tc distances for both complexes are significantly longer than the average Tc–Tc distance of 2.365(1) Å for a variety of di-μ-oxo Tc^{IV} or Tc^{IV}/Tc^{III} dimers (Table 9) where metal–metal multiple bonding has been proposed. These shorter Tc–Tc bond lengths are also reflected in the smaller Tc–O–Tc angles of these complexes, compared to those of **1** and **2**. The Tc≡N distances for complexes **1** and **2** are similar to that of 1.604(6) reported for $[TcN(S_2CNEt_2)_2]$ and those reported for other nitridotechnetium complexes.[34] Unfortunately, the Tc≡N distances of 1.65(2) and 1.59(2) Å for **2** have large e.s.d.s and this precludes any useful comparison. The weighted average Tc^{VI}–S bond lengths of 2.433(1) and 2.444(3) Å for complexes **1** and **2**, respectively, are significantly longer than that of 2.401(1) Å for Tc^{V}–S in $[TcN(S_2CNEt_2)_2]$.[22]

The geometry of the dithiocarbamate ligands is normal and similar to that in $[Mo_2O_4(S_2CNEt_2)_2]$.[33] It is of interest

Table 9 Comparative structural data for some complexes containing the TcO_2Tc core[a]

Complex	Tc–Tc/Å	Tc–O_{br}/Å	Tc–(O)–Tc/°	Ref.
1 $[\{Tc^{VI}N(S_2CNEt_2)\}_2(\mu\text{-}O)_2]$	2.543(1)	1.939(2)	82.0(1)	This work
2 $[\{Tc^{VI}N(S_2CNC_4H_8)\}_2(\mu\text{-}O)_2]$	2.542(2)	1.940(6)	81.9(4)	This work
$[(Tc^{VI}OMe_2)_2(\mu\text{-}O)_2]$	2.562(1)	1.911(1)	84.19(5)	36
$Ba_2[\{Tc(tcta)\}_2(\mu\text{-}O)_2][ClO_4]\cdot 9H_2O$[b]	2.402(1)	1.938(4)	76.7(1)	37
$Na_2[\{Tc^{IV}[N(CH_2CO_2)_3]\}_2(\mu\text{-}O)_2]\cdot 6H_2O$	2.363(2)	1.919(2)	76.0(1)	38
$[\{Tc^{IV}(H_2edta)\}_2(\mu\text{-}O)_2]\cdot 5H_2O$[c]	2.331(1)	1.913(3)	75.2(1)	39
$K_4[\{Tc^{IV}(ox)_2\}_2(\mu\text{-}O)_2]\cdot 3H_2O$	2.361(1)	1.913(1)	75.7(3)	40

[a] Bond distances and angles listed are, where appropriate, weighted mean values. [b] tcta = 1,4,7-Triazacyclononane-*N*,*N*′,*N*″-triacetate. This complex contains mixed valence technetium(III)/(IV). [c] H_2edta = Ethylenediaminetetraacetate(2−).

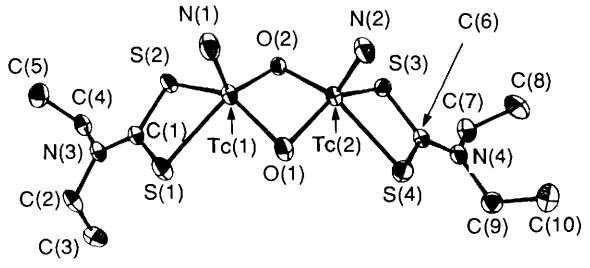

Fig. 3 An ORTEP diagram of $[\{TcN(S_2CNEt_2)\}_2(\mu\text{-}O)_2]$ **1** showing 30% probability ellipsoids

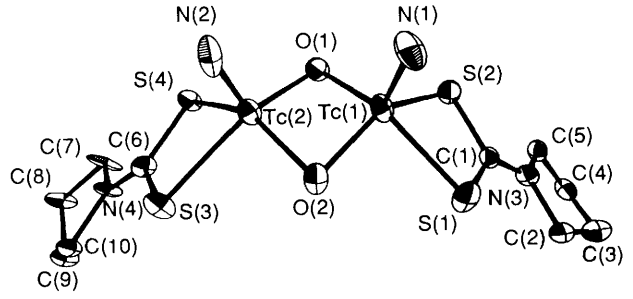

Fig. 4 An ORTEP diagram of $[\{TcN(S_2CNC_4H_8)\}_2(\mu\text{-}O)_2]$ **2** showing 30% probability ellipsoids

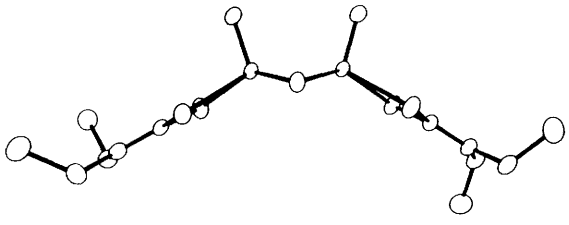

Fig. 5 A perspective view of the *syn* isomer **1**, showing the dihedral angle (*ca.* 151°) between the two TcO_2 planes

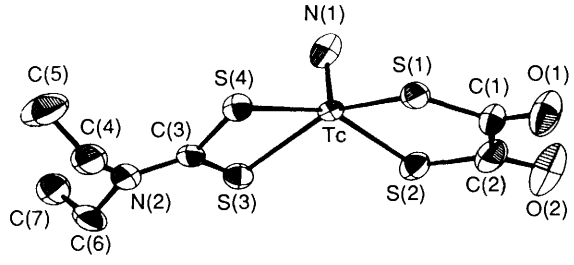

Fig. 6 An ORTEP diagram of $[AsPh_4][TcN(S_2CNEt_2)(SCOCOS)]$ **3** showing 30% probability ellipsoids

that three methyl groups of the dithiocarbamate ligands in complex **1** are aligned in the same direction as the Tc≡N bond, whereas the remaining methyl group is not. This situation is the same as that found in the oxomolybdenum analogue, but distinctly different from that observed in $[TcN(S_2CNEt_2)_2]$ where only two of the methyl groups of the dithiocarbamate ligands align with the Tc≡N bond. Also, one of the S_2CNC_2 fragments in **1** comprising atoms S(3), S(4), N(4), C(6), C(7), C(9) is essentially planar (χ^2 258), while that of S(1), S(2), N(3), C(1), C(2), C(4) is less so (χ^2 1541). This contrasts with $[TcN(S_2CNEt_2)_2]$ where both S_2CNC_2 fragments are planar.

The pyrrolidinyl groups in complex **2** show a distinct puckering of the NC_4 rings. However, if atoms C(4) and C(9) are omitted from the plane calculation, the remaining atoms of the pyrrolidinyl group are planar with the C(4) and C(9) atoms being displaced by 0.41(2) and 0.56(2) Å from their respective planes.

$[AsPh_4][TcN(S_2CNEt_2)(SCOCOS)]$ **3**. Complex **3** consists of discrete $[AsPh_4]^+$ cations and $[TcN(S_2CNEt_2)(SCOCOS)]^-$ anions. A perspective view of the anion including the atom numbering is shown in Fig. 6. The technetium atom is in a distorted square-pyramidal environment, with the nitrido ligand in the apical position. The metal is displaced by 0.66(1) Å above the S_4 basal plane.

The dithiooxalate ligand in **3** is planar (χ^2 9) with a maximum deviation of 0.05 Å. The dithiocarbamate ligand has both methyl groups aligned in the direction of the Tc≡N bond and the S_2CNC_2 fragment is planar (χ^2 15). The dihedral angle of *ca.* 150° between the normals of the dithiooxalate ligand and the S_2CNC_2 fragment renders a butterfly conformation to the anion, as is generally found for a variety of five-co-ordinate technetium complexes.[34] The weighted mean Tc–S distance of 2.394(3) Å is similar to that of 2.401(1) Å for $[TcN(S_2CNEt_2)_2]$[22] and 2.387(1) Å for $[AsPh_4]_2(TcN(SCOCOS)_2]$.[18a] It should be noted that a lack of good quality crystals for **3** enabled only a poor structure refinement, and consequently some of the reported bond lengths and angles are at best only approximate. Thus, the Tc≡N length of 1.54(2) Å, although noticeably shorter than is generally found for nitridotechnetium complexes, has a large e.s.d. and comparisons are therefore not meaningful.

It is of particular interest to examine structural influences of the oxo (O^{2-}) and nitrido (N^{3-}) ligands in related complexes. Previously, we have compared structural aspects in pairs of technetium complexes which differ only by the presence of TcN^{2+} or TcO^{3+} cores.[41] While the electronic (π) influence of the nitrido ligand was seen to be greater than that of the oxo ligand, as evidenced by NTc–S bond distances being longer than OTc–S distances, the technetium atoms in the oxo complexes are displaced further from the basal plane, suggesting that the oxo ligand exerts the larger steric effect. The present structure analyses allow a comparison of the nitrido and oxo ligands in monomeric and dimeric complexes containing the isoelectronic cores TcN^{2+} and MoO^{2+} and TcN^{3+} and MoO^{3+}.

Comparative structural data for closely related monomeric complexes containing the isoelectronic TcN^{2+} and MoO^{2+} cores are given in Table 10. Clearly, for purposes of comparing the rather small differences in detail that result from changing between isoelectronic cores, the present structure determination of **3** is inadequate on two counts: the structure analysis is of insufficient quality, and the complex, containing both a

Table 10 Comparative structural data for square-pyramidal complexes of dithiocarbamato ligands containing TcN^{2+} and MoO^{2+} cores; sbp denotes the square basal plane

Complex	Tc≡N or Mo=O/Å	M–S/Å	N– or O–M–S/°	M–sbp/Å	Ref.
$[TcN(S_2CNEt_2)_2]$	1.604(6)	2.392(2)–2.405(2)	107.0(2)–108.9(2)	0.75	22
$[TcN(S_2CNEt_2)(SCOCOS)]$	1.54(2)	2.374(6)–2.424(5)	103.7(6)–107.3(6)	0.66	This work
$[MoO(S_2CNPr^n_2)_2]$	1.664(8)	2.410(2)–2.418(2)	108.3(2)–111.7(2)	0.83	42

Table 11 Comparative structural data for dimeric complexes containing isoelectronic TcN^{3+} and MoO^{3+} cores; sbp denotes the square basal plane

Complex	Tc≡N or Mo=O/Å	M–M/Å	M–S/Å	M–O_{br}/Å	M–sbp/Å	Ref.
1 $[\{TcN(S_2CNEt_2)\}_2(\mu\text{-}O)_2]$	1.623(4) 1.624(4)	2.543(1)	2.428(1)–2.436(1)	1.935(3)–1.942(3)	0.65(1) 0.65(1)	This work
2 $[\{TcN(S_2CNC_4H_8)\}_2(\mu\text{-}O)_2]$	1.65(2) 1.59(2)	2.542(2)	2.437(6)–2.457(5)	1.934(13)–1.947(12)	0.65(1) 0.67(1)	This work
$[\{MoO(S_2CNEt_2)\}_2(\mu\text{-}O)_2]$	1.677(2) 1.680(2)	2.580(1)	2.447(1)–2.459(1)	1.940(2)–1.943(2)	0.73	33

dithiocarbamate and a 1,2-dithiolate ligand, is too dissimilar to the others.

Restricting the comparison to $[TcN(S_2CNEt_2)_2]$[22] and $[MoO(S_2CNPr^n_2)_2]$,[42] in the isoelectronic TcN^{2+} and MoO^{2+} cores the Tc^{V}≡N distance is considerably less than Mo^{IV}=O but this may simply reflect σ-bonding effects.[41] Unlike the case of complexes containing the TcN^{2+} and TcO^{3+} cores, where NTc–S bond distances are longer than OTc–S distances,[41] here there is no evidence for the nitrido ligand exerting a stronger π-electronic effect, with OMo^{IV}–S distances being slightly longer than NTc^{V}–S distances. This is possibly a result of the different oxidation states of the metals. However, as previously observed,[41] the oxo ligand exhibits a greater steric effect than the nitrido ligand, with molybdenum displaced more from the basal plane and O=Mo–S angles generally greater than the N≡Tc–S angles.

It is of interest to make similar comparisons in the cases of the dimeric TcN^{3+} species **1** and **2** and the dimeric MoO^{3+} complex $[\{MoO(S_2CNEt_2)\}_2(\mu\text{-}O)_2]$.[33] Comparative structural data for these dimeric complexes are given in Table 11. Again there is no evidence in the M–S and M–O bond distances for any difference in electronic effects of the isoelectronic TcN^{3+} and MoO^{3+} cores. The oxo ligand again appears to exert the greater steric effect with the molybdenum atoms displaced more from the basal plane than the technetium atoms in the nitrido-technetium dimers.

ESR measurements may give evidence for differences between the electronic effects in TcN^{3+} and MoO^{3+} cores in monomeric complexes. However, these differences appear to be small. The spin densities in the ligand p orbitals for $[MoOCl_5]^{2-}$, as calculated by Manoharan and Rogers,[43] are assumed to be the same for $[MoOCl_4]^{-}$, and are slightly larger than those calculated for $[TcNCl_4]^{-}$ (6% as against 5.2% respectively).[30] Similarly, the isotropic chloride superhyperfine interaction, calculated from the frozen solution results following Shock and Rogers,[44] is 2×10^{-4} cm^{-1} for $[TcNCl_2(S_2CNEt_2)]$, which may be compared with the value of 2.3×10^{-4} cm^{-1} for the analogous $[MoOCl_2(S_2CNEt_2)]$ complex reported by Larin *et al.*[45]

The present work has shown that di-μ-oxo $Tc^{VI}N$ species are stable and may be readily isolated. The cleavage of the di-μ-oxo dimers to give singly bridged μ-oxo dimers, and the equilibrium between these and the monomer, have been confirmed by preliminary extended X-ray absorption fine structure studies in acid solutions. These results will be reported shortly.

References

1 E. I. Stiefel, *Prog. Inorg. Chem.*, 1977, **22**, 1.
2 B. Spivack and Z. Dori, *Coord. Chem. Rev.*, 1975, **17**, 99.
3 C. D. Garner and J. M. Charnock, in *Comprehensive Coordination Chemistry*, eds. G. Wilkinson, R. D. Gillard and J. A. McCleverty, Pergamon, Oxford, 1987, vol. 3, p. 1329.
4 J. Baldas, J. F. Boas, J. Bonnyman, S. F. Colmanet and G. A. Williams, *Inorg. Chim. Acta*, 1991, **179**, 151.
5 J. Baldas, J. F. Boas, J. Bonnyman, S. F. Colmanet and G. A. Williams, *J. Chem. Soc., Chem. Commun.*, 1990, 1163.
6 J. Baldas, S. F. Colmanet and M. F. Mackay, *J. Chem. Soc., Dalton Trans.*, 1988, 1725.
7 J. Baldas, J. Bonnyman and G. A. Williams, *Inorg. Chem.*, 1986, **25**, 150.
8 J. Baldas, J. F. Boas and J. Bonnyman, *Aust. J. Chem.*, 1989, **42**, 639.
9 D. F. Grant, E. J. Gabe and Y. Le Page, GLSOR Least Squares Orientation Matrix Program, National Research Council of Canada, Ottawa, 1978.
10 D. T. Cromer and D. Liberman, *J. Chem. Phys.*, 1970, **53**, 1891.
11 G. M. Sheldrick, in *Crystallographic Computing 3*, eds. G. M. Sheldrick, C. Krüger and R. Goddard, Oxford University Press, 1985.
12 G. M. Sheldrick, Program for Crystal Structure Determination, University of Cambridge, 1976.
13 D. T. Cromer and J. B. Mann, *Acta Crystallogr., Sect. A*, 1968, **24**, 321.
14 *International Tables for X-Ray Crystallography*, eds. J. A. Ibers and W. C. Hamilton, Kynoch Press, Birmingham, 1974, vol. 4, p. 100.
15 R. F. Stewart, E. R. Davidson and W. T. Simpson, *J. Chem. Phys.*, 1965, **42**, 3175.
16 C. K. Johnson, ORTEP II, Fortran Thermal-Ellipsoid Plot Program, Oak Ridge National Laboratories, TN, 1976.
17 J. Baldas, J. F. Boas, S. F. Colmanet and M. F. Mackay, *Inorg. Chim. Acta*, 1990, **170**, 233.
18 (*a*) S. F. Colmanet and M. F. Mackay, *Inorg. Chim. Acta*, 1988, **147**, 173; (*b*) J. Baldas and J. Bonnyman, *Inorg. Chim. Acta*, 1988, **141**, 153.
19 C. M. Archer, J. R. Dilworth, J. D. Kelly and M. McPartlin, *J. Chem. Soc., Chem. Commun.*, 1989, 375.
20 M. J. Clarke and J. Lu, in *Technetium and Rhenium in Chemistry and Nuclear Medicine 3*, eds. M. Nicolini, G. Bandoli and U. Mazzi, Raven Press, New York, 1990, p. 23.
21 G. J.-J. Chen, J. W. McDonald, D. C. Bravard and W. E. Newton, *Inorg. Chem.*, 1985, **24**, 2327.
22 J. Baldas, J. Bonnyman, P. M. Pojer, G. A. Williams and M. F. Mackay, *J. Chem. Soc., Dalton Trans.*, 1981, 1798.
23 K. M. Harmon and R. R. Lake, *Inorg. Chem.*, 1968, **7**, 1921.
24 I. G. Dance, A. G. Wedd and I. W. Boyd, *Aust. J. Chem.*, 1978, **31**, 519.
25 S. F. Colmanet, G. A. Williams and M. F. Mackay, *J. Chem. Soc., Dalton Trans.*, 1987, 2305.
26 J. Baldas, S. F. Colmanet and M. F. Mackay, *J. Chem. Soc., Chem. Commun.*, 1989, 1890; J. Baldas and S. F. Colmanet, *Inorg. Chim. Acta*, 1990, **176**, 1.
27 R. Barral, C. Bocard, I. Sérée de Roch and L. Sajus, *Tetrahedron Lett.*, 1972, 1693.
28 W. E. Newton, J. L. Corbin, D. C. Bravard, J. E. Searles and J. W. McDonald, *Inorg. Chem.*, 1974, **13**, 1100.
29 S. E. Lincoln and T. M. Loehr, *Inorg. Chem.*, 1990, **29**, 1907.
30 J. Baldas, J. F. Boas, S. F. Colmanet and G. A. Williams, *J. Chem. Soc., Dalton Trans.*, 1991, 2441.

31 M. I. Scullane, R. D. Taylor, M. Minelli, J. T. Spence, K. Yamanouchi, J. H. Enemark and N. D. Chasteen, *Inorg. Chem.*, 1979, **18**, 3213.
32 D. Collison, F. E. Mabbs, J. H. Enemark and W. E. Cleland, jun., *Polyhedron*, 1986, **5**, 423.
33 L. Ricard, C. Martin, R. Wiest and R. Weiss, *Inorg. Chem.*, 1975, **14**, 2300.
34 S. F. Colmanet and G. A. Williams, in *Technetium and Rhenium in Chemistry and Nuclear Medicine 3*, eds. M. Nicolini, G. Bandoli and U. Mazzi, Raven Press, New York, 1990, p. 55.
35 B. Jezowska-Trzebiatowska, M. J. Rudolf, L. Natkaniec and H. Sabat, *Inorg. Chem.*, 1974, **13**, 617; T. Chandler, D. L. Lichtenberger and J. H. Enemark, *Inorg. Chem.*, 1981, **20**, 75.
36 W. A. Herrmann, R. Alberto, P. Kiprof and F. Baumgärtner, *Angew. Chem., Int. Ed. Engl.*, 1990, **29**, 189.
37 K. E. Linder, J. C. Dewan and A. Davison, *Inorg. Chem.*, 1989, **28**, 3820.
38 G. Anderegg, E. Müller, K. Zollinger and H. B. Bürgi, *Helv. Chim. Acta*, 1983, **66**, 1593.
39 H. B. Bürgi, G. Anderegg and P. Bläuenstein, *Inorg. Chem.*, 1981, **20**, 3829.
40 R. Alberto, G. Anderegg and A. Albinati, *Inorg. Chim. Acta*, 1990, **178**, 125.
41 G. A. Williams and J. Baldas, *Aust. J. Chem.*, 1989, **42**, 875.
42 L. Ricard, J. Estienne, P. Karagiannidis, P. Toledano, J. Fischer, A. Mitschler and R. Weiss, *J. Coord. Chem.*, 1974, **3**, 277.
43 P. T. Manoharan and M. T. Rogers, *J. Chem. Phys.*, 1968, **49**, 5510.
44 J. R. Shock and M. T. Rogers, *J. Chem. Phys.*, 1973, **58**, 3356.
45 G. M. Larin, M. K. Tuiebaev, G. A. Zvereva, V. V. Minin, D. Kh. Kamysbaev, *Russ. J. Inorg. Chem. (Engl. Transl.)*, 1990, **35**, 858.

Received 13*th March* 1992; *Paper* 2/01358D